Journal of Catalysis **203,** 393–406 (2001)
doi:10.1006/jcat.2001.3320, available online at http://www.idealibrary.com on IDEAL®

Role of the Ceria–Zirconia Support in the Reactivity of Platinum and Palladium Catalysts for Methane Total Oxidation under Lean Conditions

Christine Bozo,* Nolven Guilhaume,*,[1,2] and Jean-Marie Herrmann†

*Laboratoire d'Application de la Chimie à l'Environnement (UMR 5634), Université Claude Bernard Lyon 1, Bât. 303, 43 Boulevard du 11 Novembre 1918, F-69622 Villeurbanne Cedex, France; and †IFoS (UMR 5621), Equipe Photocatalyse, Catalyse et Environnement, Ecole Centrale de Lyon, BP 163, F-69131 Ecully Cedex, France

Received March 12, 2001; revised June 21, 2001; accepted June 22, 2001

Platinum or palladium catalysts deposited on a $Ce_{0.67}Zr_{0.33}O_2$ solid solution were tested in methane total oxidation. The ceria–zirconia mixed oxide is itself an active catalyst for methane combustion, in the 673–1073 K temperature range. Deposition of platinum or palladium on this support results in a strong increase in activity, which now takes place at low temperature (473–773 K). The ceria–zirconia support is particularly beneficial for the activity of platinum, when compared to a Pt/Al_2O_3 catalyst. Methane oxidation takes place at the active ceria–zirconia/metal interface, according to a redox mechanism involving the reaction of dissociated methane with lattice oxygen from the support. However, a time-on-stream deactivation is observed at moderate temperatures (573–623 K), which is associated with an oxidized state of the catalysts, whereas a reduction at 573 K strongly activates the solids. *In situ* **electrical conductivity measurements show that the reduction at 573 K of the $Pt/Ce_{0.67}Zr_{0.33}O_2$ and $Pd/Ce_{0.67}Zr_{0.33}O_2$ catalysts creates a large amount of oxygen vacancies. Although the reduced ceria–zirconia support is largely reoxidized by oxygen at 573 K, some vacancies still remain and require a higher oxidation temperature (773 K) to be filled. The presence of vacancies, even in small amounts, seems to favor activity because of an electron transfer to the noble metals and an improvement of the lattice oxygen mobility. The slow filling of these vacancies is probably an important factor contributing to the observed time-on-stream deactivation.** © 2001 Academic Press

Key Words: **ceria–zirconia solid solutions; methane combustion; platinum; palladium; electrical conductivity; oxygen vacancies; metal–support interactions; SMSI.**

INTRODUCTION

Ceria–zirconia solid solutions tend to replace ceria as oxygen storage components in the recent generation of three-way catalysts. Compared to pure ceria, ceria–zirconia solid solutions have improved oxygen storage capacity (OSC) and thermal stability (1). Whereas the OSC of ceria depends directly on its surface area, the ceria–zirconia mixed oxides are able to maintain high OSC despite severe sintering (2). This property is believed to be related to the displacement of the oxygen sublattice around zirconium, leading to a higher oxygen mobility and an easier bulk reduction of the solid solutions (3, 4).

The oxygen mobility in ceria or ceria–zirconia supports is important for three-way catalysis, since the oxygen from the support becomes available for the oxidation of CO or hydrocarbons when the air/fuel ratio becomes reducing ("rich" composition). Furthermore, the reduction of the support creates oxygen vacancies, and these vacancies play an important role in the activity. They provide sites for oxygen activation by formation of superoxide (O_2^-) and peroxide species (O_2^{2-}) (5). Several types of superoxide species were identified by EPR on ceria (6, 7) and ceria–zirconia mixed oxides (8). According to energy calculations (9), the presence of oxygen vacancies also promotes the oxidation of CO on the (110) and (310) surfaces of CeO_2. NO also reacts at 373 K with oxygen vacancies of ceria to produce N_2O (10).

The effect of ceria addition on the activity of noble metals has been mostly studied in the CO oxidation reaction, often under reducing conditions, in view of a better understanding of the role of ceria in three-way catalysts as oxygen supplier under fuel-rich conditions. The use of ceria as a support in place of alumina for Pt, Pd, and Rh has been shown to promote CO oxidation at low temperature, particularly for Pt/CeO_2 (11). In addition to a reaction mechanism identical to that occurring on bulk metals or alumina-supported catalysts, a second mechanism was evidenced under reducing conditions and at low temperature (473 K), which involves oxygen from the ceria lattice. This second mechanism also operates over a $Pd/Ce_{0.5}Zr_{0.5}O_2$ catalyst, with a rate 2–3 times higher than that over a Pd/CeO_2 catalyst treated in the same conditions

[1] To whom correspondence should be addressed. E-mail: guilhaum@catalyse.univ-lyon1.fr.

[2] Present address: Institut de Recherches sur la Catalyse, 2 Av. Albert Einstein, F-69626 Villeurbanne Cedex, France.

0021-9517/01 $35.00

(12). Methane steam reforming on Pd/CeO_2 also involves the reaction of oxygen from ceria with dissociated methane on palladium (13). Several authors have also stressed the participation of oxygen from ceria's lattice in the activity (14, 15).

As regards the oxidation of hydrocarbons under oxidizing conditions, several studies have shown either no effect of ceria on the activity of noble metals or a negative one. In the case of methane total oxidation, Oh *et al.* (16) observed a detrimental effect of ceria on the activity of platinum and palladium, whereas the activity of a Rh catalyst remained unchanged. Hicks *et al.* (17) draw the same conclusions for methane oxidation with Pd/Al_2O_3 catalysts doped with ceria, as did Shyu *et al.* (18) for propane oxidation. Groppi *et al.* (19) investigated the effect of ceria addition on the activity of Pd/La_2O_3-stabilized Al_2O_3 in high temperature methane combustion under lean conditions: ceria does not significantly affect the light-off performance but stabilizes PdO toward its reduction at high temperature. The same effect of ceria (increase in CO oxidation activity, but no effect on CH_4 oxidation) is also observed with $Cu/Ce/Al_2O_3$ catalysts (20).

Tiernan and Finlayson (21), however, put these results into perspective in their work on the effect of ceria on $Pt/Ce–Al_2O_3$ catalysts used for the total oxidation of isobutane. A negative effect of the addition of ceria on the activity is indeed observed with solids calcined in air, but after a reduction at 773 K, or an activation in a stoichiometric $i–C_4H_{10}/O_2$ mixture, the ceria-containing catalysts become more active than Pt/Al_2O_3. Many authors have also observed that a prereduction of noble metal–ceria catalysts results in an improved activity (22–26). A strong but transient increase in NO conversion in the (NO + CO) reaction was also observed after reduction of a $Rh/Ce_{0.5}Zr_{0.5}O_2$ catalyst at 473 K (27). A $Rh/Ce–Al_2O_3$ TWC, deactivated in air at 1073 K, can be regenerated by reduction in H_2 at the same temperature (28). This activation slowly falls off upon exposure to oxygen-rich reaction conditions (26), by oxidative pretreatment (23) or with time-on-stream (27). Several authors attribute this deactivation to the oxidation of the noble metals (23, 24, 26). Ceria is known for its ability to promote the oxidation of noble metals and their stabilization in an oxidized state (29), because of the very high redox potential of the Ce^{4+}/Ce^{3+} couple (1.61 eV), which is higher than those of the Rh^{3+}/Rh^0, Pt^{2+}/Pt^0, and Pd^{2+}/Pd^0 couples.

Noble metals in a reduced state, however, do not seem to be the sole condition for a high activity. The formation of oxygen vacancies by reduction of the support, in close vicinity to the metal particles (26, 30), appears to be essential to obtain activated catalysts. A low or moderate temperature reduction is yet more efficient in improving the activity than a high temperature reduction (473–573 K against 773 K in (30)), probably because a high temperature reduction induces strong metal–support interactions (SMSI effect).

Ceria–zirconia solid solutions have been scarcely used in catalytic combustion. They are themselves active for the combustion of methane, in the 673–1073 K temperature range (31, 32). Their activity is enhanced by doping the ceria–zirconia solid solutions with Mn or Cu (33). Pd–Ce–Zr–O mixed oxides, prepared by coprecipitation, were compared to a $Pd/Ce_{0.8}Zr_{0.2}O_2$ catalyst in which the palladium was deposited on the preformed support (34). This study focused on the effect of the calcination temperature (723–1473 K) on the activity in methane combustion. The supported catalysts behave better at low temperature, as expected from their higher surface Pd content. However, the drop in activity in the 950–1050 K temperature domain, due to the decomposition of PdO, is less important with the Pd-containing mixed oxides, presumably because the palladium is stabilized in an oxidized form.

The aim of the present work was to investigate the catalytic properties of Pt and Pd catalysts supported on a ceria–zirconia solid solution in methane total oxidation. In a previous paper (35), we presented preliminary results concerning the combustion of propene and methane on a $Pt/Ce_{0.67}Zr_{0.33}O_2$ catalyst. A time-on-stream deactivation of the catalyst was observed with both hydrocarbons, which was related to a poisoning by carbonates in the case of propene combustion at low temperature (423 K). For methane combustion, however, the deactivation is not due to carbonate poisoning. The present paper describes our further investigations on the activity of Pt and Pd/ceria–zirconia catalysts in methane combustion. *In situ* electrical conductivity measurements were used to try to clarify the role of oxygen vacancies of the ceria–zirconia support in the activity, in relation to the observed deactivations.

EXPERIMENTAL

The preparation and characterization of the ceria–zirconia support and the $Pt/Ce_{0.67}Zr_{0.33}O_2$ catalyst have been reported previously (35). The choice of the solid solution composition was determined on the basis of a previous study (32), in which the reducibility and the thermal stability upon aging of several $Ce_{1-x}Zr_xO_2$ solid solutions were evaluated. The $Pd/Ce_{0.67}Zr_{0.33}O_2$ catalyst was prepared by impregnation of $Pd(NH_3)_4(NO_3)_2$ on the same ceria–zirconia support. Chlorinated precursors were excluded from all the preparations, since chlorine modifies the redox properties of ceria (36) and ceria–zirconia supports (37).

The specific surface areas were measured by nitrogen adsorption at 77 K using the multipoint method. The samples were previously treated at 673 K under vacuum (2×10^{-3} Pa) for 2 h. The metal accessible areas were determined by volumetric H_2 chemisorption at 298 K under

static conditions. The catalysts were pretreated under H_2 at 573 K for 1 h, evacuated under vacuum at the same temperature to eliminate the water produced, and then reduced again under H_2 at 573 K for 15 h. The solids were evacuated at 573 K for 1 h and then cooled at 298 K before starting the H_2 chemisorption measurements. This procedure allows a sufficient reduction of the ceria–zirconia support to ensure that hydrogen is afterward consumed by chemisorption on the metals and not by reduction of the support. The metal dispersions were deduced from the irreversible H_2 uptake, calculated from the difference between total and reversible chemisorption, and an H/M_s stoichiometry of 1/1 was assumed.

Activity measurements were performed on two different apparatuses, using 0.50 g of catalyst. On the first one, the activity is measured under isothermal conditions. The temperature is raised from 473 to 873 K by steps of 50 K, the catalyst being kept at each temperature for 3 h, during which the activity is measured. The analysis is ensured by online gas chromatography, using an FID detector equipped with a Ni-catalyst methanator, which allows for the detection of CH_4, CO, and CO_2. The complete chromatographic analysis allows one their repetition every 30 min. The experiments presented in Figs. 2 and 6 were obtained with another apparatus, equipped with IR analyzers for CO, CO_2 and CH_4, and one paramagnetism analyzer for O_2. A computer drives the different sections (gas supply, temperature program) and collects the data at short time intervals (every 12 s in the experiments presented here).

Electrical Conductivity Measurements

The electrical resistance of the samples was measured with an ohmmeter (Kontron, Model DMM 4021) for $R < 2 \times 10^6\ \Omega$ (dc voltage = 1 V) or with a teraohmmeter (Guildline Instruments, Model 9520) for $10^6 > R > 10^{14}\ \Omega$ (dc voltage = 1 to 10 V). The electrical conductivity σ of a powder sample can be expressed as

$$\sigma = \frac{1}{R} \cdot \frac{t}{S},$$

where R is the electrical resistance, t is the thickness of the sample, and S is the section area of the electrodes (diameter 1.0 cm). The samples (≈900 mg) were placed between two platinum electrodes and slightly compressed (ca. 10^5 Pa) to ensure good electrical contacts between the grains. To control the temperature, both electrodes were soldered to thermocouples whose wires were also used, when short-circuited, to measure the electrical resistance. This static cell is contained in a quartz cell that allows for the treatment of samples and the introduction of gases. A general description of this static cell has been given elsewhere (38). Prior to each measurement, the samples were pretreated under oxygen at 500°C (1 h), followed by evacuation under vacuum at the same temperature.

For (semi)quantitative comparisons of the electrical conductivity of various supported samples, it is required that solids have similar textures and identical surface states. This requirement is here fulfilled since all the samples have the same $Ce_{0.67}Zr_{0.33}O_2$ support. The $Pt/Ce_{0.67}Zr_{0.33}O_2$ and $Pd/Ce_{0.67}Zr_{0.33}O_2$ catalysts have a metal loading of ≈2 wt%, which is much lower than the percolation threshold (39) above which the conductivity is governed by the most conductive phase. As a consequence, the conductivity measured is essentially that of the $Ce_{0.67}Zr_{0.33}O_2$ support. Information on the interactions between Pt or Pd and the ceria–zirconia support can be deduced by comparison with the bare support.

RESULTS

General Characteristics and Methane Combustion Activity of the Solids

The surface areas, Pt and Pd loading, and dispersions of the two catalysts are presented in Table 1.

The X-ray diffraction pattern of the $Ce_{0.67}Zr_{0.33}O_2$ support, calcined at 973 K, presents the diffraction lines of a cubic solid solution. This pattern is not modified after Pt or Pd impregnation. In addition, the $Pt/Ce_{0.67}Zr_{0.33}O_2$ pattern shows the main diffraction line of Pt^0. The intensity of this line is weak, however, and its width gives an estimated Pt particle size of 36 nm. This large size is not in agreement with H_2-chemisorption measurements, which correspond to an average Pt particle size of ≈3 nm. The Pt dispersion seems to be somewhat heterogeneous, with the presence of some large platinum particles.

No diffraction lines corresponding to metallic palladium can be seen in the pattern of $Pd/Ce_{0.67}Zr_{0.33}O_2$.

The activity of the three solids for methane total oxidation in the presence of an excess oxygen is shown on Fig. 1. Prior to the activity measurements, the $Ce_{0.67}Zr_{0.33}O_2$ support was oxidized at 673 K (1 h), whereas $Pt/Ce_{0.67}Zr_{0.33}O_2$ and $Pd/Ce_{0.67}Zr_{0.33}O_2$ catalysts were reduced at 573 K (1 h) under H_2, according to our standard pretreatments for oxide or supported noble metal catalysts, respectively. The bare Ceria–zirconia support is fairly active, with the conversion of methane initiating at 673 K and being total at

TABLE 1

Characteristics of the $Pt/Ce_{0.67}Zr_{0.33}O_2$ and $Pd/Ce_{0.67}Zr_{0.33}O_2$ Catalysts

	$Pt/Ce_{0.67}Zr_{0.33}O_2$	$Pd/Ce_{0.67}Zr_{0.33}O_2$
Wt% metal	1.98	1.96
Surface area ($m^2 \cdot g^{-1}$)	79	77
Metal dispersion	0.40	0.30
Metal particle size[a] (nm)	2.7	3.7

[a] Calculated from the metal dispersion.

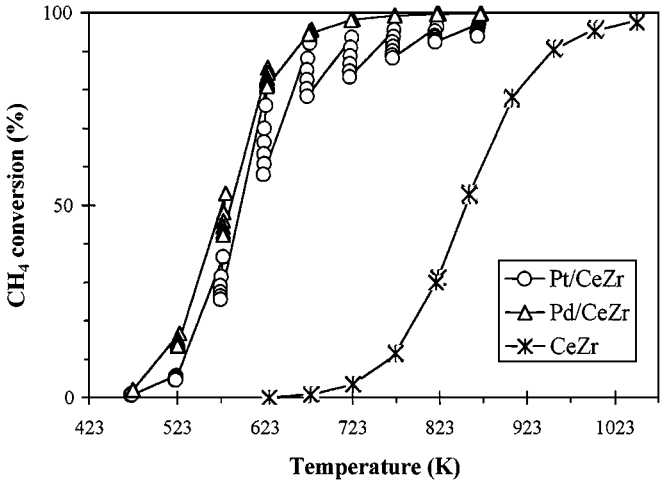

FIG. 1. Conversion of CH_4 into CO_2 as a function of temperature over $Ce_{0.67}Zr_{0.33}O_2$, $Pt/Ce_{0.67}Zr_{0.33}O_2$, and $Pd/Ce_{0.67}Zr_{0.33}O_2$. Conditions: 0.50 g catalyst, 1 vol% CH_4, 4 vol% O_2, balance N_2, total flow 6.4 $L \cdot h^{-1}$.

1073 K. In the presence of the noble metals, the activity is, as expected, strongly improved: the conversion of methane now starts at 473 K. The Pd catalyst is only slightly more active than $Pt/Ce_{0.67}Zr_{0.33}O_2$. All solids are 100% selective in CO_2.

The effect of ceria–zirconia support on the activity of the Pt and Pd catalysts can be appreciated by comparing them with Pt/Al_2O_3 and Pd/Al_2O_3 catalysts, having the same metal loading and comparable dispersions. Table 2 reports the turnover frequencies calculated on γ-Al_2O_3 and $Ce_{0.67}Zr_{0.33}O_2$ supported catalysts. The activity of platinum is clearly enhanced by the use of the $Ce_{0.67}Zr_{0.33}O_2$ support. It becomes nearly as active as palladium, and this is interesting since Pt is usually much less active than Pd for methane combustion. By contrast, the palladium activity is not modified much, whatever the support.

Under isothermal conditions, the $Pt/Ce_{0.67}Zr_{0.33}O_2$ and $Pd/Ce_{0.67}Zr_{0.33}O_2$ catalysts undergo important deactivation (i.e., the conversion over $Pt/Ce_{0.67}Zr_{0.33}O_2$ drops from 80 to 58% at 623 K in 3 h). The maximum deactivation is observed at 623 K for $Pt/Ce_{0.67}Zr_{0.33}O_2$, and at 573 K for $Pd/Ce_{0.67}Zr_{0.33}O_2$. These temperature were chosen respectively for each catalyst to study the deactivation under isothermal conditions.

TABLE 2

Comparison of Methane Oxidation Over $Ce_{0.67}Zr_{0.33}O_2$ and Al_2O_3–Supported Pt and Pd Catalysts

	Wt% metal	Metal dispersion	TOF[a] (s^{-1}) at 608 K
$Pt/Ce_{0.67}Zr_{0.33}O_2$	1.98	0.40	0.033[b]
Pt/Al_2O_3	2	0.48	0.0054
$Pd/Ce_{0.67}Zr_{0.33}O_2$	1.96	0.30	0.051[b]
Pd/Al_2O_3	2	0.26	0.071

[a] TOF = turnover frequency.
[b] Calculated at 608 K using the measured activation energy.

Previous studies on $Pt/Ce_{0.67}Zr_{0.33}O_2$ in the deactivated state allowed us to rule out some of the usual assumptions that may be considered when deactivation of catalysts under reaction condition takes place. We have shown that it is not related to any sintering of the ceria–zirconia support or the metal particles. It is also not due to a poisoning by carbonates (32). We have previously pointed out that the oxidation of propene at low temperature (423 K) involves oxygen species from the ceria–zirconia support, since poisoning of the support by surface carbonates rapidly annihilates the activity, whereas their desorption fully restores it (35). However, these surface carbonates are totally desorbed under nitrogen at low temperature (<573 K) and cannot account for the deactivation observed here with methane.

Activity of $Pt/Ce_{0.67}$ $Zr_{0.33}$ O_2 under Successive Pulses of Methane and Oxygen

To evidence the participation of oxygen from the ceria–zirconia support in methane oxidation, the activity was studied under successive sequences in flowing methane or oxygen, separated by a nitrogen flushing. Figure 2A shows the pulse sequence sent on the $Pt/Ce_{0.67}Zr_{0.33}O_2$ catalyst at 623 K (outlet O_2 and CH_4 compositions), and Fig. 2B shows the products formed and the variations of the catalyst temperature under these pulses. The sequence ($CH_4/N_2/O_2/N_2$) was repeated several times. The catalyst was previously stabilized under methane, during which the amount of CO_2 formed decreased rapidly, as the oxygen provided by the catalyst was consumed (Fig. 2B). At the end of the first step in Fig. 2B, about 45 ppm CO_2 and 110 ppm CO were still formed in the absence of gaseous oxygen.

The first important point is that a large amount of CO_2 is formed *at each transition* (N_2/CH_4 and N_2/O_2). The peak is different in shape and intensity according to the transition considered and is very reproducible.

At the N_2/O_2 transitions, when oxygen is flown to reoxidize the catalyst after the period in methane, an intense CO_2 peak (labeled ① in Fig. 2B) is observed. It corresponds to the rapid oxidation of the carbonaceous species formed on the catalyst under methane. It represent ≈55 μmol of CO_2 per gram of catalyst. This oxidation is exothermic, as can be seen by the temperature increase of the catalyst up to 629 K (Fig. 2B). This CO_2 peak is not due to the desorption of surface carbonates, since they would desorb previously during the flushing by nitrogen (they desorb readily under nitrogen at $T < 573$ K (35)). The reaction observed here is the oxidation of adsorbed CH_x species formed in the absence of oxygen at 623 K.

At the N_2/CH_4 transitions, an important CO_2 peak (labeled ② on Fig. 2B) also appears immediately, followed

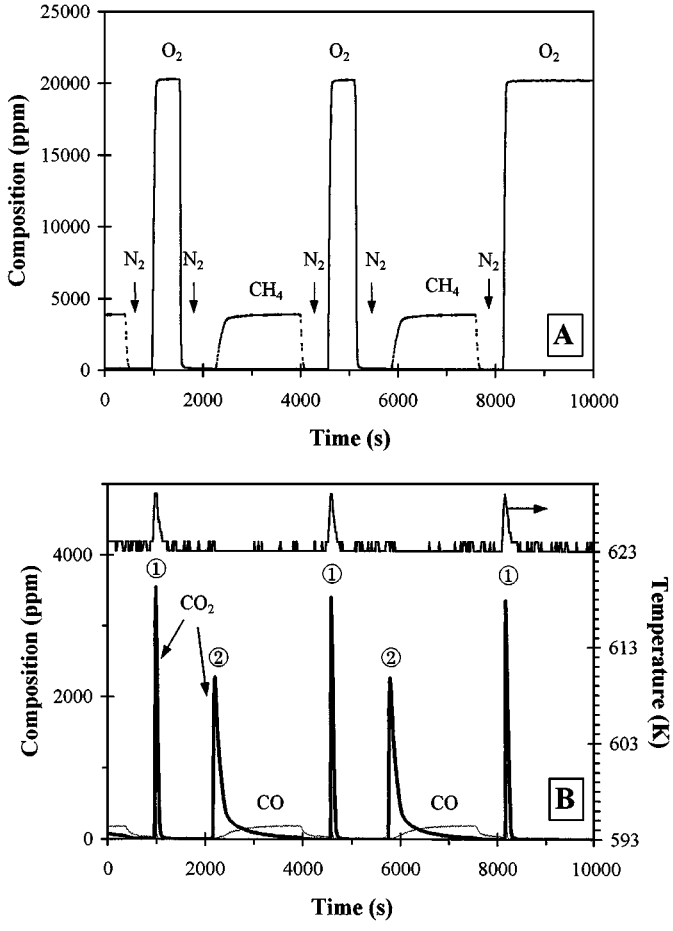

FIG. 2. Activity of $Pt/Ce_{0.67}Zr_{0.33}O_2$ under successive pulses of CH_4 and O_2. Conditions: 0.50 g catalyst, 0.4 vol% CH_4, 2 vol% O_2, balance N_2, total flow 12 L · h^{-1}. (A) Pulse sequence applied (outlet composition). (B) Products formed and temperature variations of the catalyst.

by a small amount of CO as soon as the CO_2 peak begins to decrease. It currently corresponds to methane oxidation by the oxygen supplied by the catalyst, and it represents a measure of the oxygen storage capacity at this temperature. There is no variation of the catalyst temperature during these transitions. The integration of the CO_2 and CO peaks gives an average formation of ≈127 μmol of CO_2/g of catalyst, and 68 μmol of CO/g of catalyst. Assuming a CH_4/4"O" stoichiometry for CO_2 formation,

$$CH_4 + 4\text{"}O_s\text{"} \rightarrow CO_2 + 2H_2O, \qquad [1]$$

the CO_2 peak corresponds to 508 μmol of "O"/g of catalyst. CO formation may arise from reaction with lattice oxygen with a CH_4/3"O" stoichiometry,

$$CH_4 + 3\text{"}O_s\text{"} \rightarrow CO + 2H_2O, \qquad [2]$$

which would provide an additional quantity of 204 μmol of "O"/g of catalyst. However, CO may also be formed by steam reforming of methane,

$$CH_4 + H_2O \rightarrow CO + 3H_2, \qquad [3]$$

so we cannot unequivocally ascribe the CO formed to the removal of oxygen from the catalyst. As a consequence, CO was not included in the evaluation of the oxygen storage capacity of the solid.

If we take into account the amount of oxygen coming from the oxidized surface platinum atoms ($Pt/Ce_{0.67}Zr_{0.33}O_2$ contains ≈40 μmol of exposed Pt_s atoms per gram of catalyst, which oxidize into Pt_sO under oxygen), then 10 μmol of CO_2/g from the total 127 μmol/g originate from the reaction of methane with Pt_sO. There results ca. 468 μmol of "O"/g supplied by the ceria–zirconia support. For comparison, the oxygen storage capacity of several commercial $Ce_{0.70}Zr_{0.30}O_2$ solid solutions loaded with 2 wt% Pd, measured at 623 K with CO as the reducer, varied between 390 and 570 μmol/g of catalyst after a 1323 K redox aging, but it was higher (890 μmol/g) after a simple aging in air at 873 K (40). Our results with methane are in the same range, although CO is a better reducing agent than methane.

Madier *et al.* (41) have calculated the theoretical oxygen storage capacity of ceria–zirconia solid solutions of various compositions. Assuming that there is no surface segregation of the metallic cations and an equal distribution of the (100), (110), and (111) planes, a $Ce_{0.68}Zr_{0.32}O_2$ solid solution has a theoretical OSC of 3.8 μmol of "O"/m^2. Taking the same value for our $Ce_{0.67}Zr_{0.33}O_2$ solid solution of approximately the same composition, the theoretical OSC is 300 μmol of "O"/g catalyst. This means that the reduction of the ceria–zirconia support by methane at 623 K is not restricted to the surface but also involves the removal of oxygen from the subsurface layers.

Effect of in Situ Treatments on the Isothermal Deactivation with Time-on-Stream

The left part of Fig. 3A shows the time-on-stream deactivation of both Pt and Pd catalysts, at 623 and 573 K, respectively. The solids were previously reduced in H_2 at 573 K, cooled at 473 K, and tested at 473, 523, and 573 K for 3 h at each temperature (i.e., under the same test conditions as in Fig. 1.) At 623 K ($Pt/e_{0.67}Zr_{0.33}O_2$) or 573 K ($Pd/Ce_{0.67}Zr_{0.33}O_2$), the temperature was kept constant for about 12 h. The corresponding activity decay is shown on the left part of Fig. 3: the deactivation is more pronounced with the Pt catalyst than with the Pd catalyst.

An *in situ* reduction by H_2 was then applied to both catalysts (Fig. 3A), followed by a quick flushing by nitrogen before the O_2/CH_4 mixture was admitted again. This treatment causes an outstanding activation of the two catalysts. The Pt catalyst recovers the same activity as at the beginning of the test, whereas the Pd is much

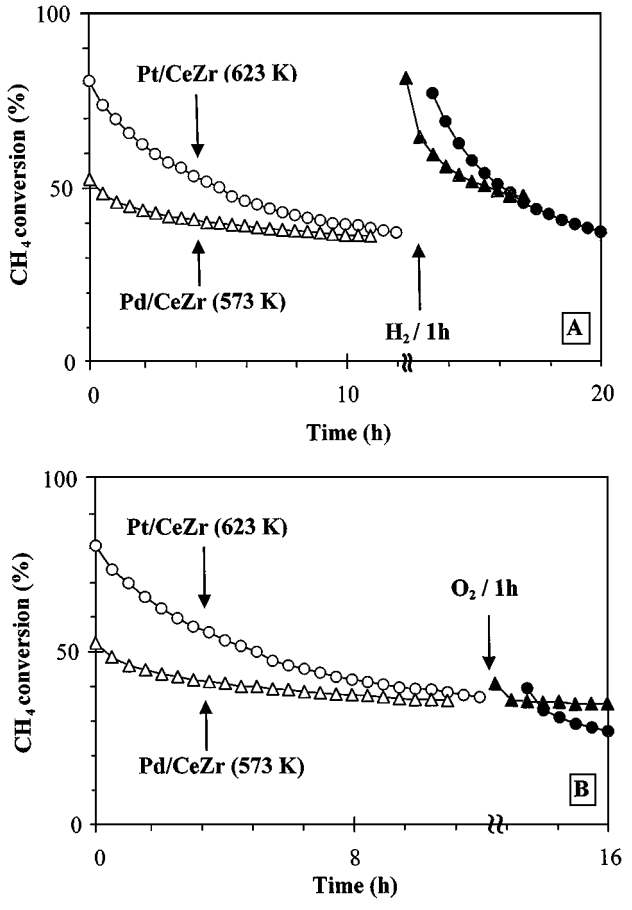

FIG. 3. Effect of *in situ* treatments on the conversion of CH_4 into CO_2 over $Pt/Ce_{0.67}Zr_{0.33}O_2$ and $Pd/Ce_{0.67}Zr_{0.33}O_2$ under isothermal conditions. (A) Effect of a reduction. (B) Effect of an oxidation. Reaction conditions: same as in Fig. 1.

more active (it becomes transiently more active at 573 K than $Pt/Ce_{0.67}Zr_{0.33}O_2$ at 623 K). The deactivation of the Pd catalyst is faster, however, particularly just after the reduction.

By contrast, an *insitu* oxidation has no effect on the deactivation profile of both catalysts (Fig. 3B). Therefore, the reduction leads to an activated state of the solids, which slowly decays under reaction conditions.

Different *in situ* treatments, shown in Fig. 4, were also applied to the $Pt/Ce_{0.67}Zr_{0.33}O_2$ catalyst. Each point represents one analysis; they are separated by a time interval of 30 min when joined by a line in the figure. When the line breaks an intermediate treatment was applied. Analyses 2 to 6 were obtained just after admitting the $O_2/CH_4/N_2$ mixture on the freshly prereduced catalyst.

During analyses 7 to 9, the oxygen concentration was doubled (8%), then brought back to its initial value (4%) in analyses 10 to 13. This has no effect on the deactivation profile, showing that the partial pressure of oxygen has no influence on the deactivation profile.

The catalyst was then oxidized at 773 K for 1 h, after which the temperature was decreased back to 623 K. A strong deactivation is now observed (analyses 18 to 20), with the conversion dropping from 60 to 37%.

Finally, a quick reduction by methane at 623 K for 15 min was applied. After this treatment, analyses 25 to 33 were obtained. This reduction allows again a remarkable reactivation of the $Pt/Ce_{0.67}Zr_{0.33}O_2$ catalyst, methane being as efficient as H_2 in this purpose.

In summary, the deactivation is a slow process in excess oxygen ($O_2/CH_4 = 4$) at 623 K, but it is much faster at 773 K. The deactivated catalyst is immediately reactivated by a quick reduction under methane.

Effect of Oxidizing or Reducing Pretreatments on the Low-Temperature Activity

Figure 5 shows the effects of successive pretreatments on the activity of the $Pt/Ce_{0.67}Zr_{0.33}O_2$ catalyst, measured under isothermal conditions at 523, 573, and 623 K in the same conditions as in Fig 1. The same catalyst was used in the three successive series of experiments. The first series (circles) shows methane conversions obtained after the standard reducing pretreatment (H_2, 573 K, 1 h). The catalyst was oxidized afterward at 773 K for 1 h, after which the second series of activity measurements (squares) is obtained. The catalyst is strongly deactivated, and this deactivation goes on, although more slowly. This deactivated sample was then reduced again by H_2 at 573 K, and the third series (triangles) is obtained. The activity is now totally restored compared to the first measurements.

Two important points appear from these experiments. First, deactivation by oxidation at 773 K is reversible: the initial activity is fully recovered when the deactivated

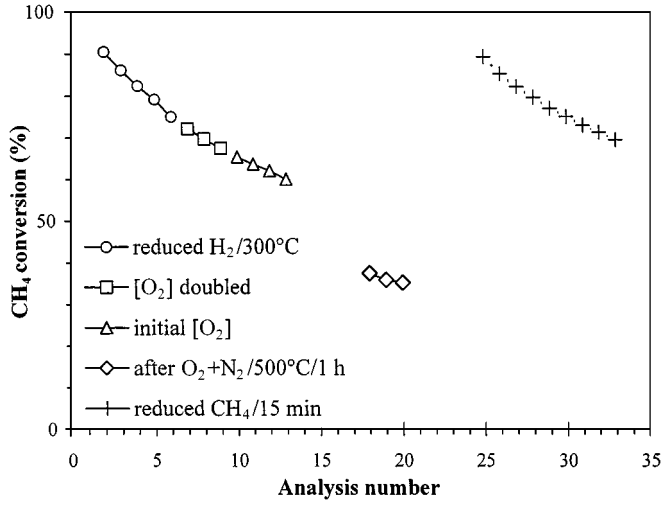

FIG. 4. Effect of *in situ* treatments on the conversion of CH_4 into CO_2 over $Pt/Ce_{0.67}Zr_{0.33}O_2$ under isothermal conditions. Reaction conditions: 623 K, same compositions as in Fig. 1.

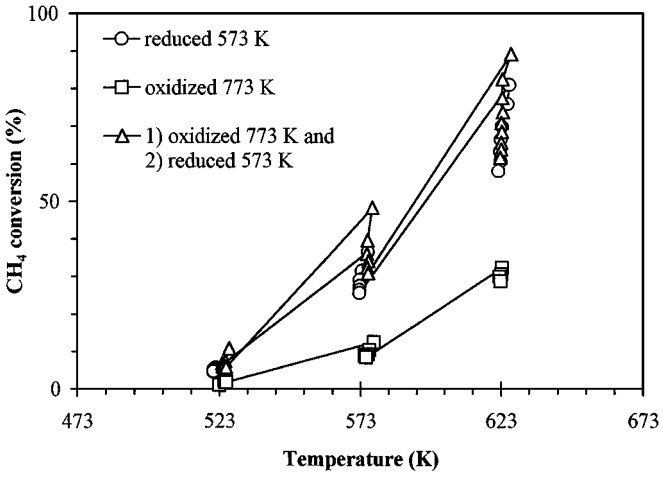

FIG. 5. Effect of pretreatments on the conversion of CH_4 into CO_2 over $Pt/Ce_{0.67}Zr_{0.33}O_2$ as a function of temperature. Reaction conditions: same as in Fig. 1.

catalyst is reduced again. This suggests that the deactivation is not related to the sintering of the metal particles or the ceria–zirconia support, as checked previously (35). Second, the reduction has a long-term effect, in the sense that it still strongly affects the activity of $Pt/Ce_{0.67}Zr_{0.33}O_2$ at 623 K, after 3 h at 523 K and 3 h at 573 K under the reactants.

Effect of the O_2/CH_4 Ratio

Since the catalysts are activated by reduction, and slowly deactivate in oxidizing conditions, the effect of increasing the O_2/CH_4 ratio on the activity of the reduced $Pt/Ce_{0.67}Zr_{0.33}O_2$ catalyst was studied. The activity is continuously monitored, with an acquisition of the data every 12 s. Figure 6A shows the effect of an increase in the oxygen partial pressure on the conversion of methane over $Pt/Ce_{0.67}Zr_{0.33}O_2$ at 623 K. In Fig. 6B, the corresponding compositions in the reaction products, CO and CO_2, are shown.

At the first step, the feedstream contains only methane, diluted in nitrogen. About 120 ppm CO_2 and 175 ppm CO are still formed in the absence of oxygen at the end of this step. It corresponds to a conversion of methane of ≈8%, which decreases rapidly (Fig. 6B).

In the following steps, increasing pressures of oxygen are introduced, but always below stoichiometry up to $O_2/CH_4 = 2$. The conversion of methane increases with oxygen concentration and reaches the maximum allowed by the amount of oxygen available in the feedstream (≈92% when $O_2/CH_4 = 1.825$). It is worth noting that only very little CO is formed even under oxygen deficiency, except at the first oxygen introduction where a CO peak briefly appears (maximum 590 ppm). This confirms the effect of the ceria–zirconia support in avoiding CO formation under rich conditions, already described in the case of ceria (29).

In the last step, the partial pressure of oxygen is set to an overstoichiometric value (close to the value of 4 used in the activity measurements). The important point is the rapid decrease of the conversion of methane as soon as the O_2/CH_4 ratio exceeds stoichiometry: the deactivation of the catalyst initiates as soon as the reaction mixture becomes oxidizing. However, at the very beginning of the last step (5200–5400 s on the time scale), the CO_2 formed (Fig. 6B) slightly exceeds the value of 4000 ppm, corresponding to the total conversion of methane (this would lead to a conversion >100% if it had been calculated on the basis of CO_2 formation). This means that there is transiently an oxidation of carbonaceous deposits, previously formed and stored on the catalyst in the absence of oxygen, which can account for the very rapid decrease in conversion at the beginning of this step. The covering of the platinum particles by oxygen, resulting in the blocking of methane adsorption and dissociation sites, also probably contributes to the initial very rapid decrease in the conversion of methane

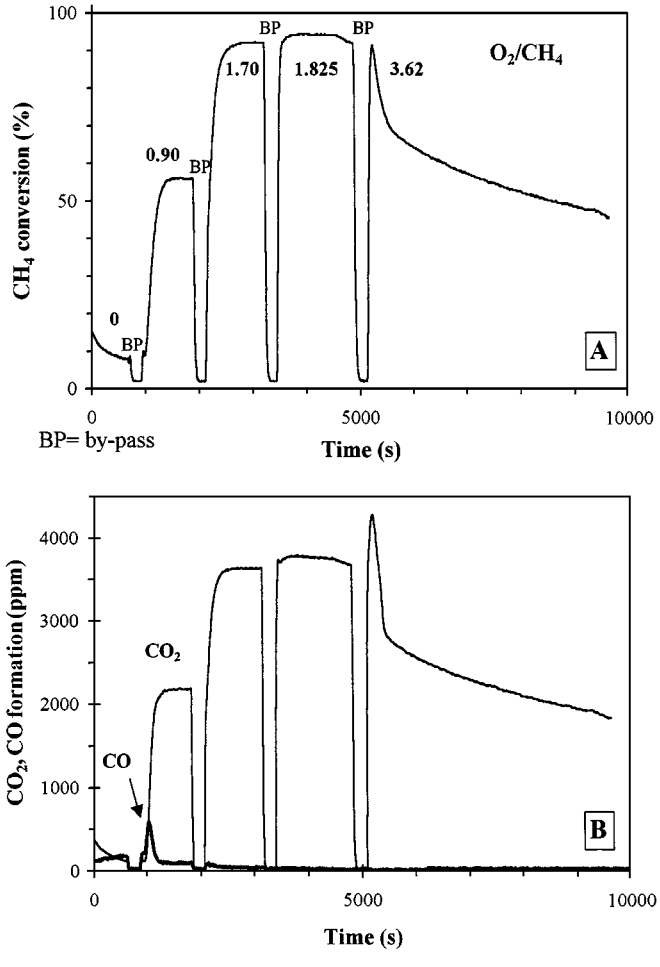

FIG. 6. Effect of the O_2/CH_4 ratio on the activity of $Pt/Ce_{0.67}Zr_{0.33}O_2$. (A) Conversion of methane. (B) Products formed. Reaction conditions: 0.50 g catalyst, 0.4 vol% CH_4, O_2 variable, balance N_2, total flow 12 L · h^{-1}.

(between 5200 and 5600 s). Afterward the activity decay becomes slower and corresponds now to that observed previously under oxidizing conditions.

Electrical Conductivity Study

Because the activation and deactivation phenomena are related to the reduced and oxidized states of the $Ce_{0.67}Zr_{0.33}O_2$-supported metal catalysts, *in situ* measurements of the electrical conductivity of the catalysts under reaction conditions were performed to obtain a better understanding of their catalytic behavior. Ceria is an n-type semiconductor, in which the conduction electrons are generated predominantly by oxygen vacancies (42, 43). The electrical properties of ceria–zirconia solid solutions have also been investigated, because of the electrochemical uses of stabilized zirconias. These studies concerned mainly Zr-rich (tetragonal) solid solutions. Chiodelli *et al.* (44) undertook a systematic study of the conduction in the whole Zr/Ce composition range and in the 473–1273 K temperature range. They showed that the conductivity is mostly ionic for tetragonal solids solutions with <30 mol% CeO_2. In contrast, it is mainly electronic for cubic, Ce-rich solid solutions (44). The main effect of Zr addition to ceria is that it broadens the conduction band, whereas almost no effects occur in the valence band and therefore on hole mobility. Quasi-free electrons become the only mobile charge carriers, at least at low temperature (<1023 K), even if their concentration is low over the holes (44).

We first measured the variations of the electrical conductivity of $Pt/Ce_{0.67}Zr_{0.33}O_2$ and $Pd/Ce_{0.67}Zr_{0.33}O_2$, as well as that of the $Ce_{0.67}Zr_{0.33}O_2$ support, as a function of temperature and oxygen pressure, to compare their behavior with literature data. Variations of the electrical conductivity under reaction mixture ($CH_4 + O_2$) after various *in situ* treatments has also been studied in relation to the catalytic activity.

The Arrhenius-type plots of the conductivity dependence on the temperature, measured in air between 473 and 923 K, is shown in Fig. 7. At $T > 573$ K, the exponential variations of the conductivity with temperature are consistent with a semiconductor behavior. Three different slopes can be distinguished. However, at low temperature (473–573 K), σ variations are indicative of nonactivated semiconductor oxides behaving as insulators. Two temperature domains close to that of catalysis can be considered for the three solids; the corresponding activation energies of conduction are reported in Table 3. Changes in the slope of $\log(\sigma) = f(1/T)$ diagrams have also been observed in the case of ceria and of cubic ceria–zirconia solid solutions (44). They reveal changes in mode of conduction (nature of the defects generating the charge carriers or mobility of these carriers). The activation energies of conduction calculated for our solids are in agreement with those obtained for cubic ceria–zirconia solid solutions (44). However, the experimental conductivity values measured for our catalysts are much lower than those reported in (44). Actually, the direct comparison of the experimental values of σ obtained with different samples is not possible, because σ depends on the purity of the samples, the shape and the size of the grains, the number of contact points, and the compression of the powder. The samples used in (44) were prepared by solid-state reaction between CeO_2 and ZrO_2 at 1873 K and have obviously very low surface areas. Therefore, the discrepancy in σ values is not unexpected. However, we can compare the conductivity values obtained on our catalysts, because they originate from the same $Ce_{0.67}Zr_{0.33}O_2$ support.

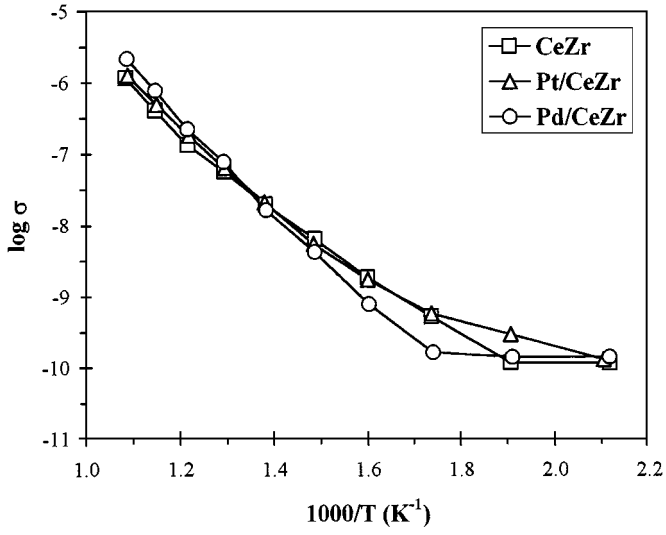

FIG. 7. Arrhenius-type plots of the electrical conductivity dependence on temperature for $Ce_{0.67}Zr_{0.33}O_2$, $Pt/Ce_{0.67}Zr_{0.33}O_2$, and $Pd/Ce_{0.67}Zr_{0.33}O_2$, measured in air.

The logarithmic plot of the variation of σ as a function of the oxygen pressure at 918 K is shown in Fig. 8. The oxygen pressure was varied between 0.013 and 0.92 atm (i.e., between 1.317 and 93.22 kPa). The conductivity decreases when the oxygen pressure increases, which is consistent with an n-type conduction where the charge carriers

TABLE 3

Activation Energies of Conduction of the Ceria–Zirconia-Based Catalysts

	Temperature domain (K)	E_c (kJ · mol^{-1})	E_c (eV)
$Ce_{0.67}Zr_{0.33}O_2$	523–773	83	0.86
	823–923	139	1.44
$Pt/Ce_{0.67}Zr_{0.33}O_2$	573–673	73	0.76
	673–923	114	1.18
$Pd/Ce_{0.67}Zr_{0.33}O_2$	573–823	122	1.26
	823–923	148	1.54

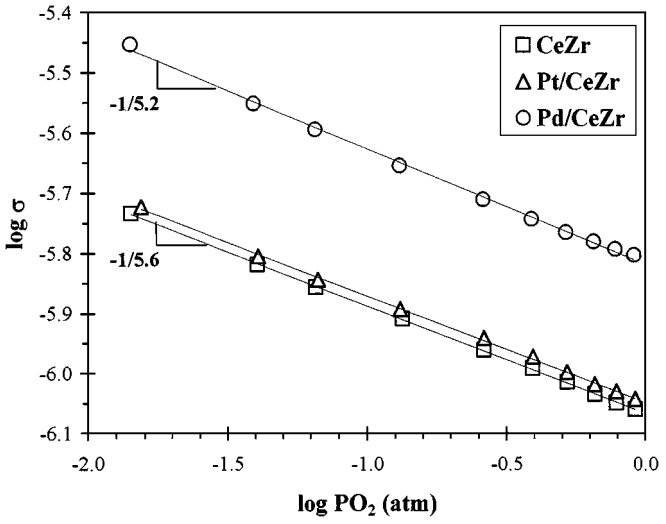

FIG. 8. Logarithmic plots of the electrical conductivity dependence of $Ce_{0.67}Zr_{0.33}O_2$, $Pt/Ce_{0.67}Zr_{0.33}O_2$, and $Pd/Ce_{0.67}Zr_{0.33}O_2$ on the partial pressure of oxygen, measured at 918 K.

are electrons. The slopes of the straight lines fitting the data are close to $-1/6$ for $Ce_{0.67}Zr_{0.33}O_2$ and $Pt/Ce_{0.67}Zr_{0.33}O_2$ but closer to $-1/5$ for $Pd/Ce_{0.67}Zr_{0.33}O_2$. For comparison, the dependence of $\log \sigma$ as a function of $\log PO_2$ with a $Ce_{0.8}Zr_{0.2}O_2$ solid solution had slopes of $-1/4$ and $-1/5$, at 923 and 1223 K, respectively (44). $Ce_{0.67}Zr_{0.33}O_2$ and $Pt/Ce_{0.67}Zr_{0.33}O_2$ have very similar conductivity values, whereas $Pd/Ce_{0.67}Zr_{0.33}O_2$ is more conductive under similar conditions. It should be recalled that, in the methane combustion measurements, the oxygen partial pressure in the $CH_4/O_2/N_2$ gas mixture is 0.04 atm at 0% CH_4 conversion and 0.02 atm when the total conversion of methane is reached.

The increase of conductivity as oxygen pressure decreases is due to the formation of surface oxygen vacancies. The evolution of dioxygen from the surface creates two oxygen vacancies V_O. Each V_O contains the two electrons left by the departure of one lattice O^{2-} as atomic oxygen (Eq. [4]). V_O, with its two electrons trapped, is a neutral entity with respect to the ceria–zirconia lattice:

$$O_s^{2-} \Leftrightarrow 1/2O_{2(g)} + V_O. \qquad [4]$$

Upon thermal activation, the anionic vacancies easily loose one or two electrons, which are promoted in the conduction band and are responsible for the observed conductivity. σ varies linearly with $(PO_2)^{-1/4}$ when the predominant defects are singly ionized oxygen vacancies, whereas a dependence on $(PO_2)^{-1/6}$ is characteristic of the presence of doubly ionized oxygen vacancies (38). In our case, the oxygen pressure dependence is in good agreement with the presence of doubly ionized oxygen vacancies. These measurements show that electrons are easily liberated in the conduction band of the support, and this may be favored by electron transfer to platinum or to palladium.

The electrical conductivity of the catalysts has also been measured under a $(CH_4 + O_2)$ reaction mixture, in the same partial pressures as those in methane combustion measurements (1 vol% CH_4, 4 vol% O_2 in partial vacuum). To reproduce the activation and deactivation processes by reduction or oxidation, the same treatments were applied here. Prior to each measurement, the catalysts were pretreated at 773 K under oxygen for 1 h. The sequence applied to the solids is shown in Fig. 9. The time period for each step is 20–30 min. Because the variations of σ are of several orders of magnitude, they are given in a semilog plot.

Because the catalysts were pretreated by H_2 at 573 K prior to the methane oxidation catalytic test, the same pretreatment was presently applied (step 2). For the three solids, this reduction leads to a considerable increase in conductivity, because of formation of a large amount of oxygen vacancies. As expected, the reduction of the ceria–zirconia support at 573 K is enhanced by the presence of the noble metals. It is deeper with palladium than with platinum. This can be due to the higher amount of exposed surface Pd_s atoms ($\approx 55\,\mu mol \cdot g^{-1}$ vs $\approx 40\,\mu mol \cdot g^{-1}$ for Pt).

After reduction in H_2, the $(CH_4 + O_2)$ gas mixture (0.04 atm O_2, 0.01 atm CH_4) was admitted on the catalysts, as was done in the activity tests (step 4). In step 5, the oxygen pressure was doubled to ensure that enough oxygen was supplied to reoxidize the support. In step 6, the same $(CH_4 + O_2)$ mixture as in step 4 was introduced. The reoxidation of the ceria–zirconia support is very rapid, and the conductivity does not change substantially between steps 4 and 6. In step 7, temperature was increased to 623 K, and in step 8 the $(CH_4 + O_2)$ gas mixture was replaced by pure O_2 (0.04 atm). Interestingly, the Pt- and Pd-containing catalysts are less conductive under pure oxygen than under $(CH_4 + O_2)$, at the same temperature (623 K) and

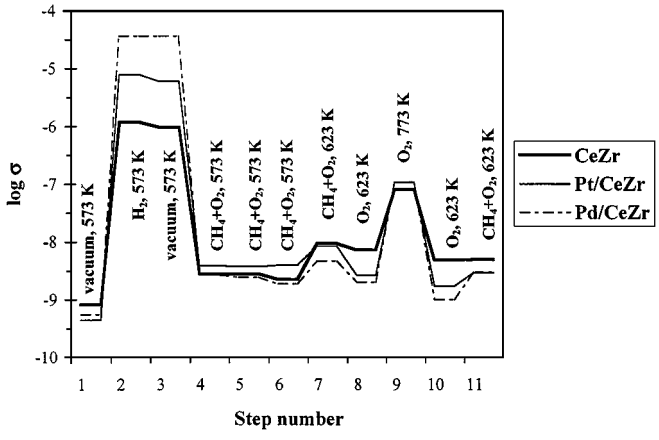

FIG. 9. Semilog plots of the variations of the electrical conductivity of $Ce_{0.67}Zr_{0.33}O_2$, $Pt/Ce_{0.67}Zr_{0.33}O_2$, and $Pd/Ce_{0.67}Zr_{0.33}O_2$ as a function of various *in situ* treatments.

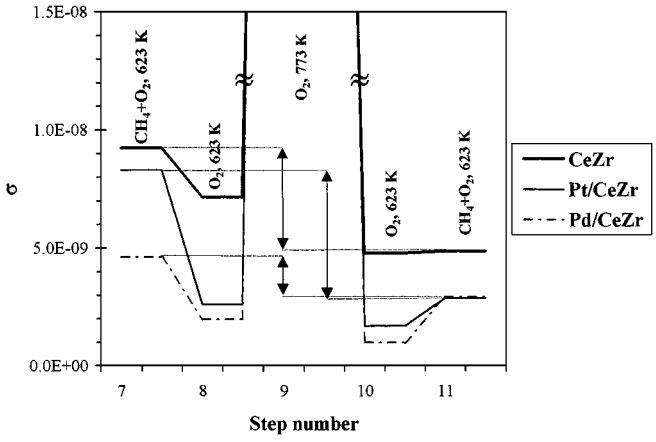

FIG. 10. Variations of the electrical conductivity of $Ce_{0.67}Zr_{0.33}O_2$, $Pt/Ce_{0.67}Zr_{0.33}O_2$, and $Pd/Ce_{0.67}Zr_{0.33}O_2$ before and after oxidation at 773 K.

under identical oxygen partial pressure. This means that, under reaction conditions ($CH_4 + O_2$), more vacancies are present than under pure oxygen. On the opposite side, the conductivity hardly changes under ($CH_4 + O_2$) or O_2 with the bare $Ce_{0.67}Zr_{0.33}O_2$ support, which is not active at 623 K (cf. Fig. 1). This supports the proposed reaction mechanism, in which lattice oxygen of the ceria–zirconia solid solution participates in the oxidation of methane.

We have seen previously (cf. Fig. 4) that oxidation at 773 K induces a strong deactivation of the catalysts. The same treatment was applied here, by heating to 773 K under oxygen for 1 h (step 9), before cooling to 623 K under the same oxygen pressure (step 10). A zoom of this sequence is shown in Fig. 10, with the conductivity no longer plotted on a logarithmic scale but with normal units ($\Omega^{-1} \cdot cm^{-1}$). The conductivity of the three solids measured under O_2 at 623 K is always lower after the treatment at 773 K. This means that, although the catalysts have been previously in contact with an excess of oxygen at 573 and 623 K, oxidation at 773 K induces an additional disappearance of some oxygen vacancies.

Eventually, the ($CH_4 + O_2$) gas mixture was introduced again at 623 K (step 11). The σ values are now lower than those measured before oxidation at 773 K, as indicated by the vertical arrows in Fig. 10. This difference is higher for $Pt/Ce_{0.67}Zr_{0.33}O_2$ than for $Pd/Ce_{0.67}Zr_{0.33}O_2$. This is in agreement with the fact that deactivation is less pronounced with the Pd catalyst. The conductivity of the $Ce_{0.67}Zr_{0.33}O_2$ support also decreases after the 773 K oxidation, but its activity in methane combustion is negligible at this temperature.

These results strongly support the idea that the deactivation of the $Ce_{0.67}Zr_{0.33}O_2$-based catalysts is related to a decrease in oxygen vacancies concentration in the ceria–zirconia support. This would also correspond to a decrease or loss of electronic transfer from the ceria–zirconia support to the noble metals.

DISCUSSION

The ceria–zirconia support is active in methane combustion, which means that methane may react with chemisorbed oxygen, or with lattice oxygen from the mixed oxide. Ceria and ceria–zirconia solid solutions can activate oxygen as superoxide and peroxide species (peroxides form only on reduced samples, because they show a higher electron-donor ability). However, these species are only observed at low temperature (<373 K), whereas activity is observed in the 673–1073 K temperature range. Nevertheless, although their residence time on the ceria surface is too short, at high temperatures, to allow their spectroscopic characterization, they have been proposed to participate in the oxygen isotopic exchange processes in ceria (45) and ceria–zirconia mixed oxides (41). There is a controversy about the reactivity of the superoxide species in oxidation reactions over ceria–containing catalysts: they are sometimes considered as active oxygen species for CO oxidation, at least at low temperature (<423 K) (6, 46). Fernandez-Garcia *et al.* (47), however, have shown that superoxide radicals adsorbed on Ce^{4+} ions do not react with CO adsorbed on Pt at 423 K and consider that the active oxygen species for CO oxidation is rather more reduced, diamagnetic oxide anions (O^{2-}) at the metal–ceria interface (47). In the same way, Li *et al.* (48) propose that the active species for ethylene oxidation over ceria is not superoxide, but lattice oxygen from ceria. Haneda *et al.* (49) also conclude that adsorbed superoxide ions require activation through the ceria lattice, with lattice oxygen being the main active species in methane oxidation.

In the presence of noble metals, the activity is enhanced and initiates now at very low temperature. In particular, the light-off temperature with the $Pt/Ce_{0.67}Zr_{0.33}O_2$ catalyst is remarkably low. The promotion effect of the ceria–zirconia support, compared to an alumina support (Table 2), is really significant with platinum, whose activity is 6 times higher on the $Ce_{0.67}Zr_{0.33}O_2$ support. With palladium, intrinsically more active for methane oxidation, the activity is slightly lower with the ceria–zirconia support. Naturally, the turnover frequency of $Pt/Ce_{0.67}Zr_{0.33}O_2$ was calculated considering the average size of the Pt particles (2.7 nm), based on hydrogen chemisorption. Some large Pt particles (>35 nm) are also present, and beacuse methane oxidation is generally considered as a structure-sensitive reaction (50, 51), this comparison has only a relative meaning. The turnover frequency would not be expected to increase so much, however, because of the sole presence of a few larger Pt particles. For comparison, the turnover frequency for methane combustion over Pt/Al_2O_3 catalysts at 608 K increases from 0.005 to 0.01 s^{-1} when the

dispersion of Pt changes from 90 to 6% (52). Therefore, the ceria–zirconia support clearly improves the activity of platinum.

In the absence of gaseous oxygen, the lattice oxygen from the ceria–zirconia support is easily removed for methane oxidation, at low temperature (623 K, Fig. 2). In the presence of an excess oxygen, methane is also oxidized by oxygen from the ceria–zirconia lattice, rather than by oxygen chemisorbed on the noble metals. An indirect proof has been given previously with the oxidation of propene under lean conditions over $Pt/Ce_{0.67}Zr_{0.33}O_2$ at low temperature (423 K): the activity was rapidly cancelled because of poisoning of the ceria–zirconia support by surface carbonates (35). The desorption of these carbonates allowed the full recovery of the high initial activity, demonstrating that the ceria–zirconia support participates in the oxidation reaction. Haneda *et al.* (53) using $CH_4 + {}^{18}O_2$ for the reaction, have shown that methane reacts selectively with lattice oxygen from ceria over $Pd/CeO_2/Al_2O_3$ catalysts. Holmgren *et al.* (30) also concluded, on the basis of the transient response of Pt/CeO_2 catalysts to $CO + {}^{18}O_2$ pulses, that the reaction of CO occurs with oxygen from ceria.

Pretreatment of the catalysts is very important in determining the initial activity. As shown in Fig. 5, a prereduction of the catalysts at moderate temperature creates a specific metal–support interaction, responsible for its high activity. Subsequently, a slow decay in activity occurs under an oxygen-rich ($CH_4 + O_2$) gas mixture, which is apparently maximum at 573–623 K. Similarly, an *in situ* reduction of the deactivated catalysts also leads to an immediate reactivation of both Pt and Pd catalysts.

The considerable activation of the $Pd/Ce_{0.67}Zr_{0.33}O_2$ catalyst on intermediate reduction (Fig. 3A) deserves some comments. PdO is often considered as more active than metallic Pd in methane combustion (54, 55). Recent studies, however, have come to the conclusions that (i) small patches of PdO formed on large, metallic Pd particles are much more active than PdO dispersed on an oxide support (56–58); and (ii) methane oxidation over PdO follows a redox mechanism, in which methane is oxidized by lattice oxygen from PdO (55). Nevertheless, the activation of methane occurs on a coordinatively unsaturated Pd site (oxygen vacancy) on the surface of a PdO crystallite, and therefore the reaction requires the presence of a Pd–PdO pair (51, 55). The highest activity is reached in the presence of both metallic Pd for methane activation and PdO for its subsequent oxidation. In our case, the considerable increase in methane conversion just after the reduction can therefore be ascribed to the easier activation of methane on metallic palladium, whereas its oxidation is ensured by oxygen from the ceria–zirconia support.

The important deactivation of the $Ce_{0.67}Zr_{0.33}O_2$-supported catalysts observed under reaction conditions can be accounted for by several possibilities: poisoning of the catalysts, modification of the catalysts, and metal–support interactions.

Poisoning of the Catalysts

Catalyst poisoning by carbonates appears as the first possibility, because of the strong basicity of ceria-based oxides. Indeed, a strong poisoning of $Pt/Ce_{0.67}Zr_{0.33}O_2$ by surface carbonates has been observed during propene oxidation at low temperature (423 K) (35). However, they were totally removed by a nitrogen flushing at 573 K. Consequently, they cannot account for the deactivation observed in methane oxidation at 623 K. The water produced by the reaction could also be a poison, but we checked that an intermediate flushing by nitrogen at 773 K, which would remove hydroxyl groups, does not allow any recovery of the activity (32). Contamination by sulfur is not possible because we used sulfur-free O_2, CH_4, and He or N_2 gases. A poisoning of the catalysts can therefore be ruled out.

Modification of the Catalysts

The sintering of the noble metals and of the ceria–zirconia support could be another reason for the observed deactivation. Therefore, the $Pt/Ce_{0.67}Zr_{0.33}O_2$ and $Pd/Ce_{0.67}Zr_{0.33}O_2$ catalysts were characterized in the deactivated state (i.e., after a 12-h period under ($CH_4 + O_2$) at 923 K). There was not a very significant sintering of the support, because the surfaces areas of the catalysts were now 77 $m^2 \cdot g^{-1}$ for $Pt/Ce_{0.67}Zr_{0.33}O_2$ and 74 $m^2 \cdot g^{-1}$ for $Pd/Ce_{0.67}Zr_{0.33}O_2$, very close to the values obtained for fresh catalysts (see Table 1). This is not unexpected because the ceria–zirconia support was previously calcined at 973 K. H_2-chemisorption measurements showed that the metal dispersions of the deactivated catalysts are not modified compared to the fresh ones. There is also no loss of metals, according to the chemical analyses. Therefore, there is no evidence for modification of the catalysts in the deactivated state.

Role of Metal–Support Interactions

Recently, metal–ceria interactions have been widely studied, because of their relevance to three-way catalysis, and comprehensively reviewed (59). Strong metal–support interactions are created by reduction of reducible supports (TiO_2, CeO_2), and they are strongly dependent on the reduction temperature. Upon reduction of M/CeO_2 catalysts (M = noble metals) at $T > 773$ K, the chemisorption as well as catalytic properties of the metals are severely disturbed but can be recovered by a mild oxidation treatment.

In our case, an opposite effect was observed: activated $Pt/Ce_{0.67}Zr_{0.33}O_2$ and $Pd/Ce_{0.67}Zr_{0.33}O_2$ catalysts are obtained after a mild reduction, whereas the deactivation occurs slowly under oxidizing conditions at moderate temperatures (573–623 K), and faster upon reduction at 773 K.

What was observed is the loss, under oxidizing conditions, of beneficial metal support interactions induced by the reduction. Therefore, it was necessary to understand the effects of reduction/oxidation on the properties of our catalysts.

As shown clearly by Bernal *et al.* (59), reduction or oxidation of M/CeO_2 catalysts at $T < 773$ K do not induce any significant microstructural changes, provided that the catalysts were previously calcined at higher temperatures. A partial covering of metal particles by ceria has been evidenced only at reduction temperatures $\geq$873 K (59). Similarly, our characterizations of the deactivated catalysts enabled us to rule out any covering or encapsulation of the metals by the ceria–zirconia support.

Ceria–zirconia solid solutions are much more reducible than pure ceria. The presence of noble metals, which dissociate H_2, promotes the reduction of the $Ce_{0.67}Zr_{0.33}O_2$ support: at room temperature, several layers of Ce^{4+} are already reduced by H_2 (35). After reduction at 573 K, the $Ce_{0.67}Zr_{0.33}O_2$ support is deeply reduced. The electrical conductivity (Fig. 9) shows an outstanding increase upon reduction: more than 3 orders of magnitude for $Ce_{0.67}Zr_{0.33}O_2$ and more than 4 orders of magnitude for $Pt/Ce_{0.67}Zr_{0.33}O_2$ and $Pd/Ce_{0.67}Zr_{0.33}O_2$. It also evidences two important points: (i) the presence of oxygen vacancies in the $Ce_{0.67}Zr_{0.33}O_2$ support, in equilibrium with gaseous oxygen, whose number increases under ($CH_4 + O_2$) reaction mixture; and (ii) the decrease in conductivity induced by oxidation at 773 K (Fig. 10). This means that part of vacancies present after a treatment under ($CH_4 + O_2$) at 623 K are irreversibly filled only upon oxidation at this temperature.

The presence of oxygen vacancies, even under oxidizing conditions, can be explained by considering the nanocrystalline nature of the $Ce_{0.67}Zr_{0.33}O_2$ support. Ranga Rao *et al.* (60) studied the reoxidation of a $Rh/Ce_{0.5}Zr_{0.5}O_2$ catalyst by NO at 473 K, following its reduction at 673 K, by XANES and magnetic susceptibility. They concluded that the ceria–zirconia support is completely reoxidized after this treatment. These measurements were performed on low surface area samples (1–2 $m^2 \cdot g^{-1}$), corresponding to large particles. By contrast, Fally *et al.* (61) studied the reoxidation of several high surface area $Ce_{1-x}Zr_xO_2$ solid solutions ($x = 0$–0.5), previously reduced at 973 K. After reoxidation of the solids at 298 K, magnetism measurements evidenced a residual amount of Ce^{3+} between 1.3 and 9.9%, according to the composition of the solid. After reoxidation at 823 K, still about 1% Ce^{3+} remains in all the solids. This amount, however, is within the accuracy limits of the technique. Rossignol *et al.* (62) also evidenced the presence, under gaseous oxygen, of reduced centers in ceria–zirconia mixed oxides.

Ceria is fundamentally nonstoichiometric oxide, in line with its n-type semiconductivity. At low oxygen pressures (10^{-2}–10^{-26} atm) and high temperatures (1023–1773 K), ceria may exhibit large deviations from stoichiometry ($x = 0.001$ to 0.3 in CeO_{2-x}) (42). In ceria powders classically prepared by precipitation, there is nearly no deviation from stoichiometry under standard conditions, but it may increase for small particle sizes. As an example, Nachimuthu *et al.* (63) studied by XANES various ceria samples with particle sizes ranging from 2 to 75 nm. All the ceria samples contained a minimum of 5% Ce^{3+} as an impurity, whereas the Ce^{3+} content was maximum for particles of 15 nm. Special synthesis conditions may also contribute to the stabilization of nonstoichiometric ceria particles. Magneton sputtering and inert gas condensation, followed by controlled oxidation, have been successfully used to prepare stable, oxygen-deficient nanocrystalline CeO_{2-x} particles (<10 nm), in which the Ce^{3+} content may reach $\approx$20% and are stable against reoxidation up to 573–673 K (64). In another approach, Haneda *et al.* (65) synthesized substoichiometric CeO_{2-x} ($x \approx 0.2$) particles deposited on alumina by a sol–gel method, followed by high-temperature reduction (1173 K). The ceria–alumina interaction was held responsible for the stabilization of Ce^{3+}, and these oxygen-deficient particles are stable against oxidation up to 973 K (49).

Another important point to consider, regarding the oxygen vacancies in the $Ce_{0.67}Zr_{0.33}O_2$ support, is the presence of platinum or palladium. The metal–ceria interaction has been sometimes interpreted within the metal/oxide junction effect theory (66). Theoretical calculations (67) suggest that the metal promotes the oxide by enhancing the equilibrium concentration of oxygen vacancies: electron transfer from the oxide to the noble metal results in a lowering of the effective activation energy for the formation of oxygen vacancies. Thus, the presence of Pt or Pd may enhance the number of oxygen vacancies. This is what we observe on Fig. 10: under oxygen, the conductivity of the bare $Ce_{0.67}Zr_{0.33}O_2$ support is always higher than in the presence of Pt and Pd, because of electron transfer from the support to the noble metals. Moreover, under the same oxygen partial pressure and in the presence of methane, the catalysts are always more conductive than under oxygen only, thus showing the presence of a higher number of vacancies under reaction conditions.

The presence of oxygen vacancies appears to be the key point of the high activity obtained after reduction. A clear relationship between oxygen deficiency in ceria and a high catalytic activity for oxidation reactions has been already established by several authors. A nonstoichiometric $Pd/CeO_{2-x}/Al_2O_3$ catalyst had a better OSC and a higher catalytic activity for methane total oxidation than stoichiometric $Pd/CeO_2/Al_2O_3$ (65). The kinetics for methane total oxidation also exhibit significant differences. EPR measurements reveal that superoxide species are formed on all catalysts, but in a much larger amount on CeO_{2-x}/Al_2O_3 (53). The authors propose that, with the nonstoichiometric support, the superoxide species are rapidly activated by

diffusion into the CeO_{2-x} surface vicinity and converted into lattice oxygen, which is the active oxygen species. Actually, the role of the oxygen defects would be to improve oxygen activation and mobility. Tschöpe *et al.* (64) also pointed out the importance of nonstoichiometry for CO and CH_4 oxidation over La and Cu-doped CeO_{2-x} catalysts.

Hence, it seems that the presence of a small amount of oxygen vacancies can strongly improve the catalytic activity of $Pt/Ce_{0.67}Zr_{0.33}O_2$. We presently think that oxygen vacancies play two important roles in the activity: (i) they promote oxygen activation and mobility in the $Ce_{0.67}Zr_{0.33}O_2$ support; and (ii) they allow the presence of quasi-free electrons, which contribute to the electronic enrichment of the noble metals. In the case of $Pd/Ce_{0.67}Zr_{0.33}O_2$, the activity is less affected by the ceria–zirconia support, because with palladium the reaction mechanism is already a redox one, involving lattice oxygen from PdO. Therefore the supply of lattice oxygen from the ceria–zirconia support is less important for the activity. The role of the oxygen vacancies of the support would be limited to an electronic transfer to palladium.

Naturally, the possibility of restructuring of the metal particles under reaction cannot be disregarded. However, some changes in the metal dispersions would be expected to occur upon reconstruction, and this is not what we observe. Moreover, redispersion of the metal crystallites is more likely to take place with palladium (68) or rhodium (69), which are easily oxidized into bulk PdO or RH_2O_3 oxides, rather than with platinum which does not form bulk oxides (70–72). Therefore, we think that the creation of oxygen vacancies upon reduction is a key point to the activation of the $Ce_{0.67}Zr_{0.33}O_2$-supported catalysts and that their slow filling under oxidizing conditions is an important factor contributing to their deactivation during methane combustion.

CONCLUSIONS

Ceria–zirconia solid solutions do not behave as simple supports in the total oxidation of methane: they are intrinsically active oxides in methane combustion. When used as supports for noble metals, they show a versatile behavior. The catalysts are activated after a reduction, or by use under a slightly reducing ($CH_4 + O_2$) reaction mixture, whereas they slowly deactivate under oxidizing conditions. The activity is the result of the cooperation between the metal, responsible for methane dissociation, and the support that supplies active lattice oxygen species. The presence of oxygen vacancies appears to be a key factor in the activity. They allow electronic transfer to the noble metals and gaseous oxygen, and they promote both mobility and lability of lattice oxygen of the ceria–zirconia support. The time-on-stream deactivation of ceria–zirconia-based methane combustion catalysts is a complex problem, which may involve several simultaneous phenomena, but the filling of the oxygen vacancies is clearly associated with it.

ACKNOWLEDGMENTS

We gratefully acknowledge GAZ DE FRANCE and ADEME for their financial support. N.G. thanks Michel Primet for his encouragement throughout this work.

REFERENCES

1. Cuif, J.-P., Blanchard, G., Touret, O., Marczi, M., and Quéméré, E., SAE Paper 961906, 1996.
2. Balducci, G., Fornasiero, P., Di Monte, R., Kaspar, J., Meriani, S., and Graziani, M., *Catal. Lett.* **33**, 193 (1995).
3. Vlaic, G., Di Monte, R., Fornasiero, P., Fonda, E., Kaspar, J., and Graziani, M., *J. Catal.* **182**, 378 (1999).
4. Fornasiero, P., Fonda, E., Di Monte, R., Vlaic, G., Kaspar, J., and Graziani, M., *J. Catal.* **187**, 177 (1999).
5. Li, C., Domen, K., Maruya, K., and Onishi, T., *J. Am. Chem. Soc.* **111**, 7683 (1989).
6. Zhang, X., and Klabunde, K. J., *Inorg. Chem.* **31**, 1706 (1992).
7. Soria, J., Martinez-Arias, A., and Conesa, J. C., *J. Chem. Soc., Faraday Trans.* **91**, 1669 (1995).
8. Martinez-Arias, A., Fernandez-Garcia, M., Ballesteros, V., Salamanca, L. N., Conesa, J. C., Otero, C., and Soria, J., *Langmuir* **15**, 4796 (1999).
9. Sayle, T. X. T., Parker, S. C., and Catlow, C. R. A., *Surface Sci.* **316**, 329 (1994).
10. Martinez-Arias, A., Soria, J., Conesa, J. C., Seoane, X. L., Arcoya, A., and Cataluña, R., *J. Chem. Soc., Faraday Trans.* **91**, 1679 (1995).
11. Bunluesin, T., Putna, E. S., and Gorte, R. J., *Catal. Lett.* **41**, 1 (1996).
12. Bunluesin, T., Gorte, R. J., and Graham, G. W., *Appl. Catal. B-Environ.* **14**, 105 (1997).
13. Craciun, R., Shereck, B., and Gorte, R. J., *Catal. Lett.* **51**, 149 (1998).
14. Jin, T., Okuhara, T., Mains, G. J., and White, J. M., *J. Phys. Chem.* **91**, 3310 (1987).
15. Hardacre, C., Ormerod, R. M., and Lambert, R. M., *J. Phys. Chem.* **98**, 10901 (1994).
16. Oh, S. H., Mitchell, P. J., and Siewert, R. M., *J. Catal.* **132**, 287 (1991).
17. Hicks, R. F., Rigano, C., and Pang, B., *Catal. Lett.* **6**, 271 (1990).
18. Shyu, J. Z., Otto, K., Watkins, W. L. H., Graham, G. W., Belitz, R. K., and Gandhi, H. S., *J. Catal.* **114**, 23 (1988).
19. Groppi, G., Cristiani, C., Lietti, L., Ramella, C., Valentini, M., and Forzatti, P., *Catal. Today* **50**, 399 (1999).
20. Park, P. W., and Ledford, J. S., *Catal. Lett.* **50**, 41 (1998).
21. Tiernan, M. J., and Finlayson, O. E., *Appl. Catal., B* **19**, 23 (1998).
22. Shyu, J. Z., and Otto, K., *J. Catal.* **115**, 16 (1989).
23. Serre, C., Garin, F., Belot, G., and Maire, G., *J. Catal.* **141**, 9 (1993).
24. Nunan, J. G., Robota, H. J., Cohn, M. J., and Bradley, S. A., *J. Catal.* **133**, 309 (1992).
25. Pirault, L., El Azami El Idrissi, D., Marécot, P., Dominguez, J. M., Mabilon, G., Prigent, M., and Barbier, J., *Stud. Surf. Sci. Catal.* **96**, 193 (1995).
26. Diwell, A. F., Rajaram, R. R., Shaw, H. A., and Truex, T. J., *Stud. Surf. Sci. Catal.* **71**, 139 (1991).
27. Fornasiero, P., Ranga Rao, G., Kaspar, J., L'Erario, F., and Graziani, M., *J. Catal.* **175**, 269 (1998).
28. Summers, J. C., and Ausen, S. A., *J. Catal.* **58**, 131 (1979).
29. Trovarelli, A., *Catal. Rev. Sci. Eng.* **38**, 439 (1996).
30. Holmgren, A., Azarnoush, F., and Fridell, E., *Appl. Catal., B* **22**, 49 (1999).

31. Zamar, F., Trovarelli, A., de Leitenburg, C., and Dolcetti, G., *J. Chem. Soc., Chem. Commun.* 965 (1995).
32. Bozo, C., Guilhaume, N., Garbowski, E., and Primet, M., *Catal. Today* **59**, 33 (2000).
33. Terribile, D., Trovarelli, A., de, Leitenburg, C., Primavera, A., and Dolcetti, G., *Catal. Today* **47**, 133 (1999).
34. Primavera, A., Trovarelli, A., de Leitenburg, C., Dolcetti, G., and Llorca, J., *Stud. Surf. Sci. Catal.* **119**, 87 (1998).
35. Bozo, C., Garbowski, E., Guilhaume, N., and Primet, M., *Stud. Surf. Sci. Catal.* **130A**, 581 (2000).
36. Bernal, S., Calvino, J. J., Cifredo, G. A., Gatica, J. M., Perez Omil, J. A., Laachir, A., and Perrichon, V., *Stud. Surf. Sci. Catal.* **96**, 275 (1995).
37. Fornasiero, P., Hickey, N., Kaspar, J., Dossi, C., Gava, D., and Graziani, M., *J. Catal.* **189**, 326 (2000).
38. Herrmann, J.-M., *in* "Catalyst Characterization: Physical Techniques for Solid Materials" (B., Imelik, and J. C., Vedrine, Eds.), p. 559. Plenum Press, New York, 1994.
39. Ovenston, A., and Walls, J. R., *J. Phys. D. Appl. Phys.* **18**, 1859 (1985).
40. Jen, H.-W., Graham, G. W., Chun, W., McCabe, R. W., Cuif, J.-P., Deutsch, S. E., and Touret, O., *Catal. Today* **50**, 309 (1999).
41. Madier, Y., Descorme, C., Le Govic, A. M., and Duprez, D., *J. Phys. Chem. B* **103**, 10999 (1999).
42. Blumenthal, R. N., *J. Solid State Chem.* **12**, 307 (1975).
43. Chang, E. K., and Blumenthal, R. N., *J. Solid State Chem.* **72**, 330 (1988).
44. Chiodelli, G., Flor, G., and Scagliotti, M., *Solid State Ionics* **91**, 109 (1996).
45. Li, C., Domen, K., Maruya, K., and Onishi, T., *J. Catal.* **123**, 436 (1990).
46. Sass, A. S., Shvets, V. A., Savel'eva, G. A., Popova, N. M., and Kazanskii, V. B., *Kinet. Catal. Engl. Transl.* **26**, 799 (1985).
47. Fernandez-Garcia, M., Martinez-Arias, A., Salamanca, L. N., Coronado, J. M., Anderson, J. A., Conesa, J. C., and Soria, J., *J. Catal.* **187**, 474 (1999).
48. Li, C., Xin, Q., and Guo, X.-X., *Catal. Lett.* **12**, 297 (1992).
49. Haneda, M., Mizushima, T., and Kakuta, N., *J. Chem. Soc., Faraday Trans.* **91**, 4459 (1995).
50. Zwinkels, M. F. M., Järås, S. G., and Menon, P. G., *Catal. Rev.—Sci. Eng.* **35**, 319 (1993).
51. Chin, Y.-H., and Resasco, D. E., *Catalysis* **14**, 1 (1999).
52. Hicks, R. F., Qi, H., Young, M. L., and Lee, R. G., *J. Catal.* **122**, 280 (1990).
53. Haneda, M., Mizushima, T., and Kakuta, N., *J. Phys. Chem. B* **102**, 6579 (1998).
54. Burch, R., and Urbano, F. J., *Appl. Catal. A-Gen.* **124**, 121 (1995).
55. Fujimoto, K., Ribeiro, F. H., Avalos-Borja, M., and Iglesia, E., *J. Catal.* **179**, 431 (1998).
56. Datye, A. K., Bravo, J., Nelson, T. R., Atanasova, P., Lyubovsky, M., and Pfefferle, L., *Appl. Catal., A* **198**, 179 (2000).
57. Hicks, R. F., Qi, H., Young, M. L., and Lee, R. G., *J. Catal.* **122**, 295 (1990).
58. Lyubowsky, M., and Pfefferle, L., *Appl. Catal. A* **173**, 107 (1998).
59. Bernal, S., Calvino, J. J., Cauqui, M. A., Gatica, J. M., Larese, C., Pérez Omil, J. A., and Pintado, J. M., *Catal. Today* **50**, 175 (1999).
60. Ranga Rao, G., Fornasiero, P., Di Monte, R., Kaspar, J., Vlaic, G., Balducci, G., Meriani, S., Gubitosa, G., Cremona, A., and Graziani, M., *J. Catal.* **162**, 1 (1996).
61. Fally, F., Perrichon, V., Vidal, H., Kaspar, J., Blanco, G., Pintado, J. M., Bernal, S., Colon, G., Daturi, M., and Lavalley, J. C., *Catal. Today* **59**, 373 (2000).
62. Rossignol, S., Gérard, F., and Duprez, D., *J. Mater. Chem.* **9**, 1615 (1999).
63. Nachimuthu, P., Shih, W.-C., Liu, R.-S., Jang, L.-Y., and Chen, J.-M., *J. Solid State Chem.* **149**, 408 (2000).
64. Tschöpe, A., Liu, W., Flytzani-Stephanopoulos, M., and Ying, J. Y., *J. Catal.* **157**, 42 (1995).
65. Haneda, M., Mizushima, T., Kakuta, N., Ueno, A., Sato, Y., Matsuura, S., Kasahara, K., and Sato, M., *Bull. Chem. Soc. Jpn.* **66**, 1279 (1993).
66. Golunski, S. E., Hatcher, H. A., Rajaram, R. R., and Truex, T. J., *Appl. Catal. B* **5**, 367 (1995).
67. Frost, J. C., *Nature* **334**, 577 (1988).
68. Hicks, R. F., Qi, H., Kooh, A. B., and Fischel, L. B., *J. Catal.* **124**, 488 (1990).
69. Chakraborti, S., Datye, A. K., and Long, N. J., *J. Catal.* **108**, 444 (1987).
70. Smith, D. J., White, D., Baird, T., and Fryer, J. R., *J. Catal.* **81**, 107 (1983).
71. McCabe, R. W., Wong, C., and Woo, H. S., *J. Catal.* **114**, 354 (1988).
72. Wang, C. B., and Heh, C. T., *J. Catal.* **178**, 450 (1998).